

## *Supporting Information*

### **The steric hindrance effect of Co porphyrins promoting two-electron oxygen reduction reaction selectivity**

Yonghong Mou,<sup>†,a</sup> Jieling Zhang,<sup>†,a</sup> Haonan Qin,<sup>a</sup> Xinyue Li,<sup>a</sup> Zequan Zeng,<sup>b</sup> Rong Zhang,<sup>b</sup> Zuozhong Liang,<sup>a,\*</sup> Rui Cao,<sup>a,\*</sup>

<sup>a</sup>Key Laboratory of Applied Surface and Colloid Chemistry, Ministry of Education, School of Chemistry and Chemical Engineering, Shaanxi Normal University, Xi'an 710119, China

<sup>b</sup>National Key Laboratory of High Efficiency and Low Carbon Utilization of Coal, Institute of Coal Chemistry, Chinese Academy of Sciences, Taiyuan 030001, China

Correspondence E-mail: [liangzuozhong@snnu.edu.cn](mailto:liangzuozhong@snnu.edu.cn), [ruicao@snnu.edu.cn](mailto:ruicao@snnu.edu.cn).

<sup>†</sup>These authors contributed equally to this work.

## **General Methods and Materials.**

Manipulations of air- and moisture-sensitive materials were performed under N<sub>2</sub> using standard Schlenk line techniques. All reagents were purchased from commercial suppliers and were used without further purification unless otherwise stated. All solvents used in these experiments were reagent grades. Dry solvents, including dichloromethane (DCM), chloroform, tetrahydrofuran (THF), and methanol were purified through activated alumina. Dimethylformamide (DMF) was dried by distillation with calcium hydride under reduced pressure. Toluene was refluxed over sodium blocks and distilled under reduced pressure. All aqueous solutions were prepared freshly using Milli-Q water. <sup>1</sup>H NMR spectra were recorded on a JEOL spectrometer operating at 400 MHz. High-resolution mass spectra (HRMS) were acquired using a Brüker MAXIS apparatus. UV-vis spectra were collected using a Hitachi U-3900H spectrophotometer.

## **Electrochemical Studies.**

All electrochemical measurements were performed using a CH Instruments (CHI 660E Electrochemical Analyzer). Cyclic voltammogram (CV) data were recorded in dry DMF containing 0.10 M Bu<sub>4</sub>NPF<sub>6</sub> and 0.50 mM catalyst with a three-compartment cell possessing a glassy carbon (GC, 0.07 cm<sup>2</sup>) electrode as the working electrode, graphite rod as the auxiliary electrode, and Ag/AgNO<sub>3</sub> as the reference electrode (BASi, 10 mM AgNO<sub>3</sub>, 0.10 M Bu<sub>4</sub>NPF<sub>6</sub> in acetonitrile). The solution was bubbled with N<sub>2</sub> for at least 30 min before analysis. GC electrode was polished with α-Al<sub>2</sub>O<sub>3</sub> of

decreasing sizes (1.0  $\mu\text{m}$  to 50 nm) and washed with distilled water (DIW) and DMF. Ferrocene was added as an internal standard. Electrocatalytic ORR measurements were performed in 0.1 M KOH solution by using Biopotentiostat (model DY2300 Electrochemical Analyzer) in a conventional three-electrode system with rotating-ring disk electrode (RRDE) or rotating disk electrode (RDE) loaded with catalysts as the working electrode, graphite rod as the auxiliary electrode, and Ag/AgCl (saturated KCl solution) as the reference electrode. The area of platinum ring electrode is 0.188  $\text{cm}^2$ , while that of GC disk electrode is 0.125  $\text{cm}^2$ . Equation 1 can be used to convert the measured potential into the electrode potential relative to the reversible hydrogen electrode (RHE).

$$E_{\text{RHE}} = E_{\text{Ag/AgCl}} + 0.197 + 0.0592 \times \text{pH} \quad (1)$$

Linear sweep voltammogram (LSV) data were measured in  $\text{O}_2$ -saturated 0.1 M KOH solutions at 5  $\text{mV s}^{-1}$ . Tafel plots were calculated by measuring LSV data at 2  $\text{mV s}^{-1}$  and 1600 rpm. The electron transfer number ( $n$ ) during ORR can be calculated from RRDE analysis.

$$n = 4 \times \frac{I_d}{I_d + \frac{I_r}{N}} \quad (2)$$

The  $n$  value can also be calculated from Koutecky-Levich (K-L) analysis.

$$\frac{1}{j} = \frac{1}{j_k} + \frac{1}{j_d} = -\frac{1}{nFkC_{\text{O}_2}} - \frac{1}{0.2nFD_{\text{O}_2}^{2/3}v^{-1/6}C_{\text{O}_2}\omega^{1/2}} \quad (3)$$

The  $I_d$  is the disk current,  $I_r$  is the ring current,  $j$  is the current density,  $j_k$  is the kinetic current density, and  $j_d$  is the diffusion-limited current density. The  $F$  is the Faraday constant (96485  $\text{C mol}^{-1}$ ),  $k$  is the rate constant of ORR,  $n$  is the number of electrons

transferred per molecule of O<sub>2</sub>, C<sub>O<sub>2</sub></sub> is the concentration of O<sub>2</sub> in 0.1 M KOH (1.26 × 10<sup>-6</sup> mol cm<sup>-3</sup>), D<sub>O<sub>2</sub></sub> is the diffusion coefficient of O<sub>2</sub> (1.90 × 10<sup>-5</sup> cm<sup>2</sup> s<sup>-1</sup>), ν is the kinematic viscosity of 0.1 M KOH (0.01 cm<sup>2</sup> s<sup>-1</sup>), and ω (rpm) is the rotation rate. In addition, the yield of hydrogen peroxide (%H<sub>2</sub>O<sub>2</sub>) can be verified by RRDE by the following Equation 4.

$$\% H_2O_2 = 200 \times \frac{\frac{I_r}{N}}{I_d + \frac{I_r}{N}} \quad (4)$$

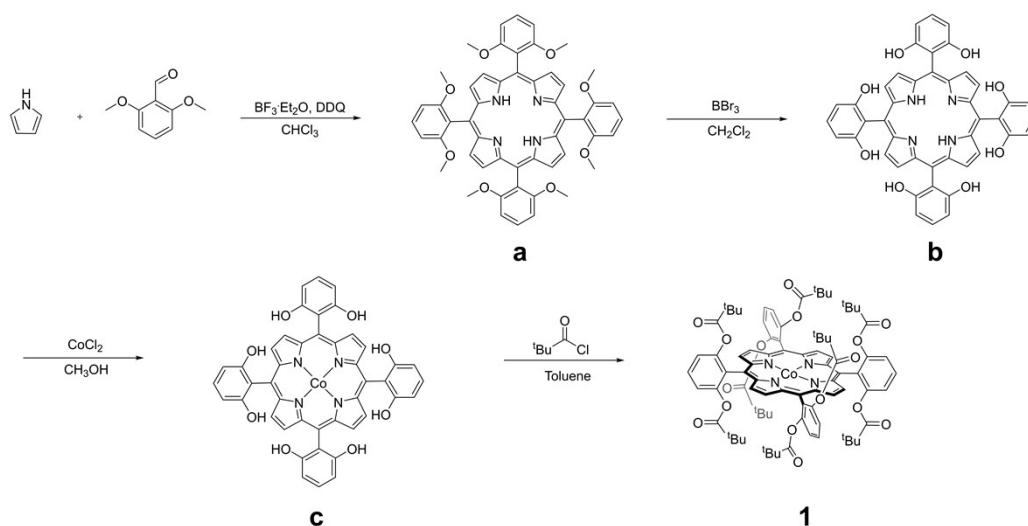
### **X-ray Diffraction Studies.**

Crystals of high quality were obtained by slow evaporation of the hexane and ether solution of Co porphyrins at room temperature under dark. Complete data sets of **1** (CCDC 2384220) and **2** (CCDC 2384221) were collected. Single crystals suitable for X-ray analysis were coated with Paratone-N oil, suspended in a small fiber loop, and placed in a cooled gas stream at 153(2) K on a Bruker D8 Venture X-ray diffractometer. Diffraction intensities were measured using graphite-monochromated Mo K $\alpha$  radiation ( $\lambda = 0.71073$  Å). Data collection, indexing, data reduction and final unit cell refinements were carried out using APEX2.<sup>[1]</sup> Absorption corrections were applied using the program SADABS.<sup>[2]</sup> Structures were solved with direct methods using SHELXS4<sup>[3]</sup> and refined against  $F^2$  on all data by full-matrix least squares with SHELXL-2014,<sup>[4]</sup> following established refinement strategies. Details of the data quality and a summary of residual values of refinements are listed in Table S1. X-ray

structures were checked using IUCr's CheckCIF routine, which resulted in no level A and B alerts.

### Synthesis of Co porphyrin 1.

The synthetic route of **1** is depicted in Scheme S1.



**Scheme S1** Synthetic route of **1**.

**Synthesis of a.** The 2,6-dimethoxybenzaldehyde (1.0 g, 6.02 mmol) and pyrrole (0.42 mL, 6.02 mmol) were dissolved in 600 mL chloroform and the solution was degassed by bubbling of nitrogen for at least 30 min. Then,  $\text{BF}_3 \cdot \text{OEt}_2$  (0.40 mL, 3.24 mmol) was added via a syringe and the reaction mixture was stirred for 1.5 h under  $\text{N}_2$ . After 2,3-dichloro-5,6-dicyano-1,4-benzoquinone (DDQ, 1.31 g, 5.78 mmol) was added, the above mixture was stirred at  $65^\circ\text{C}$  for 1.5 h. Cooled to room temperature, 1 mL of triethylamine was added to neutralize the excessive acid. The solution with red fluorescence was collected and the solvent was removed by a rotary evaporator. Crude products were purified by silica chromatography (DCM:ethyl acetate = 20:1, v/v) to

afford 154 mg (0.18 mmol, 12% yield) purple solid of **a**.  $^1\text{H NMR}$  (400 MHz,  $\text{CDCl}_3$ ):  $\delta = 8.66$  (s, 8H), 7.67 (t, 4H), 6.97 (d, 8H), 3.49 (s, 24H), -2.49 (s, 2H) (Fig. S1).

**Synthesis of b.** A solution of **a** (0.20 g, 0.23 mmol) in dry DCM was placed in ice bath. Then,  $\text{BBr}_3$  (0.70 mL, 7.48 mmol) was added. The resulting green solution was stirred for 20 h at room temperature. Ethyl acetate was added to the above suspension and then washed with  $\text{NaHCO}_3$ . The organic layer was separated, washed twice with DIW and then dried over anhydrous  $\text{Na}_2\text{SO}_4$ . The resulting solution was removed by a rotary evaporator. Crude products were purified by silica chromatography (ethyl acetate:methanol = 20:1, v/v) to afford 134 mg (0.18 mmol, 78% yield) purple solid of **b**.  $^1\text{H NMR}$  (400 MHz,  $\text{CD}_3\text{OD}$ ):  $\delta = 9.03$  (s, 8H), 7.53 (t, 4H), 6.87 (d, 8H) (Fig. S2).

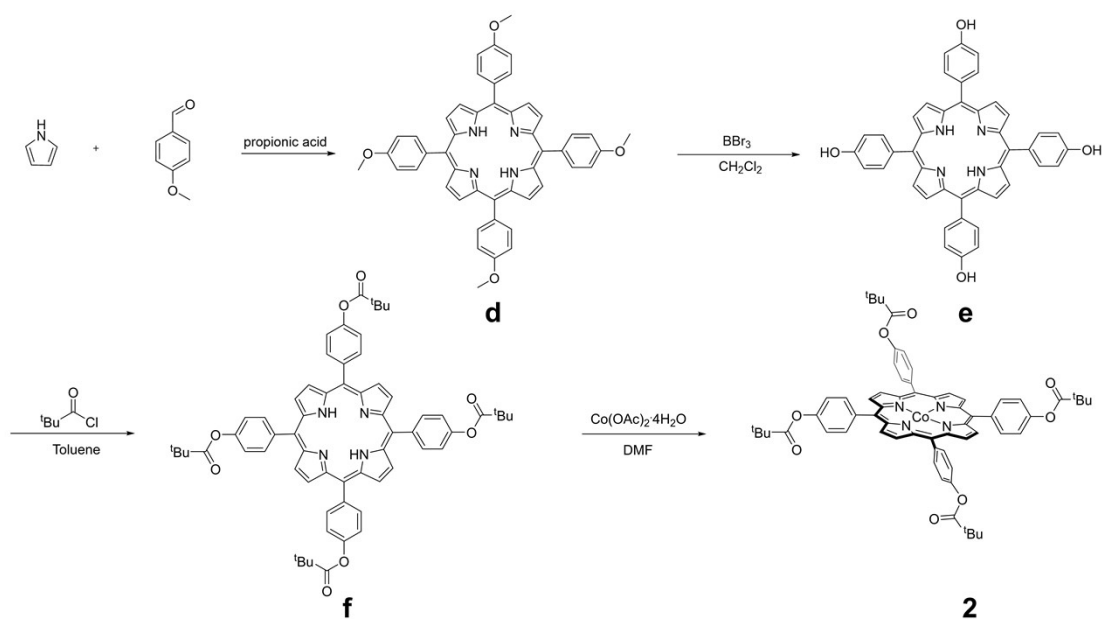
**Synthesis of c.** A solution of **b** (0.10 g, 0.13 mmol), anhydrous  $\text{CoCl}_2$  (II) (0.53 g, 4.08 mmol) and 2,6-lutidine (0.06 mL, 0.51 mmol) was mixed in dry methanol under  $\text{N}_2$  and the solution was then refluxed for 4 h. After methanol was removed, the resulting solid was dissolved in ethyl acetate, washed with DIW for three times. The organic solvent was dried over anhydrous  $\text{Na}_2\text{SO}_4$  and evaporated to give **c** as a brown solid (77 mg, 74%). HRMS of  $[\text{M} + \text{H}]^+$ : calcd.  $\text{C}_{44}\text{H}_{29}\text{CoN}_4\text{O}_8$ , 800.1312, found, 800.1305 (Fig. S3).

**Synthesis of 1.** The **c** (0.10 g, 0.12 mmol) was dissolved in a mixture of toluene/DMF/triethylamine (20 mL: 4 mL: 0.8 mL) and treated with pivaloyl chloride (1.40 mL, 11.4 mmol). After heating the mixture for 16 h under  $\text{N}_2$ , the reaction mixture was diluted with toluene (100 mL) and washed with saturated  $\text{NaHCO}_3$  (25 mL) and DIW ( $2 \times 10$  mL). The organic solvent was dried over anhydrous  $\text{Na}_2\text{SO}_4$  and removed

in a rotary evaporator. Crude products were purified by silica chromatography (DCM:ethyl acetate = 30:1, v/v) to afford 60 mg (0.04 mmol, 33% yield) brownish black solid of **1**. HRMS of  $[M + H]^+$ : calcd.  $C_{84}H_{93}CoN_4O_{16}$ , 1472.5913, found, 1472.5905 (Fig. S4).

### Synthesis of Co porphyrin **2**.

The synthetic route of **2** is depicted in Scheme S2.



**Scheme S2** Synthetic route of **2**.

**Synthesis of d.** The 4-methoxybenzaldehyde (3.65 mL, 30.0 mmol), pyrrole (2.10 mL, 20.0 mmol) were dissolved in propionic acid solution (50.0 mL) and the reaction mixture was refluxed at 120 °C for 2 h in dark. After cooling to room temperature, the resulting mixture was filtered and washed with methanol and ether. Crude products were purified by silica chromatography (hexane:ethyl acetate = 1:6, v/v) to afford 1.76 g (2.40 mmol, 8% yield) purple solid of **d**.  $^1H$  NMR (400 MHz,  $CDCl_3$ ):  $\delta$  = 8.86 (s, 8H), 8.12 (d, 8H), 7.29 (d, 8H), 4.10 (s, 12H), -2.75 (s, 2H) (Fig. S5).

**Synthesis of e.** A solution of **d** (0.20 g, 0.27 mmol) in dry DCM was placed in ice bath while  $\text{BBr}_3$  (0.22 mL, 2.36 mmol) was added. The resulting green solution was stirred for 20 h at room temperature. Ethyl acetate was added to suspension and washed with  $\text{NaHCO}_3$  (aqueous solution). The organic layer was separated, washed twice with DIW and then dried over anhydrous  $\text{Na}_2\text{SO}_4$ . The resulting solution was removed by a rotary evaporator. Crude products were purified by silica chromatography (DCM:ethyl acetate = 5:1, v/v) to afford 149 mg (0.22 mmol, 81% yield) purple solid of **e**.  $^1\text{H NMR}$  (400 MHz,  $\text{CD}_3\text{OD}$ ):  $\delta$  = 8.86 (s, 8H), 7.99 (d, 8H), 7.21 (d, 8H) (Fig. S6).

**Synthesis of f.** The **e** (0.10 g, 0.15 mmol) was dissolved in a mixture of toluene/DMF/triethylamine (20 mL: 4 mL: 0.8 mL) and treated with pivaloyl chloride (0.44 mL, 3.56 mmol). After heating the mixture for 10 h under  $\text{N}_2$ , the reaction mixture was diluted with toluene (100 mL) and washed with saturated  $\text{NaHCO}_3$  (25 mL) and DIW ( $2 \times 10$  mL). The organic solvent was dried over anhydrous  $\text{Na}_2\text{SO}_4$  and removed in a rotary evaporator. Crude products were purified by silica chromatography (DCM:ethyl acetate = 80:1, v/v) to afford 71 mg (0.07 mmol, 47% yield) purple solid of **f**.  $^1\text{H NMR}$  (400 MHz,  $\text{CDCl}_3$ ):  $\delta$  = 8.97 (s, 8H), 8.21 (d, 8H), 7.48 (d, 8H), 1.53 (s, 36H) (Fig. S7).

**Synthesis of 2.** A solution of **f** (0.10 g, 0.10 mmol),  $\text{Co}(\text{OAc})_2 \cdot 4\text{H}_2\text{O}$  (0.50 g, 2.0 mmol) and DMF (20 mL) was refluxed under inert conditions for 5 h. After cooling to room temperature, the solvent was removed by a rotary evaporator. Crude products were dissolved in DCM and washed with DIW for three times. After drying with  $\text{Na}_2\text{SO}_4$ , the products were purified by silica chromatography (DCM:ethyl acetate =



50:1, v/v) to afford 88 mg (0.08 mmol, 82% yield) dark red solid of **2**. HRMS of  $[M + H]^+$ : calcd.  $C_{64}H_{60}CoN_4O_8$ , 1072.3816, found, 1072.3814 (Fig. S8).

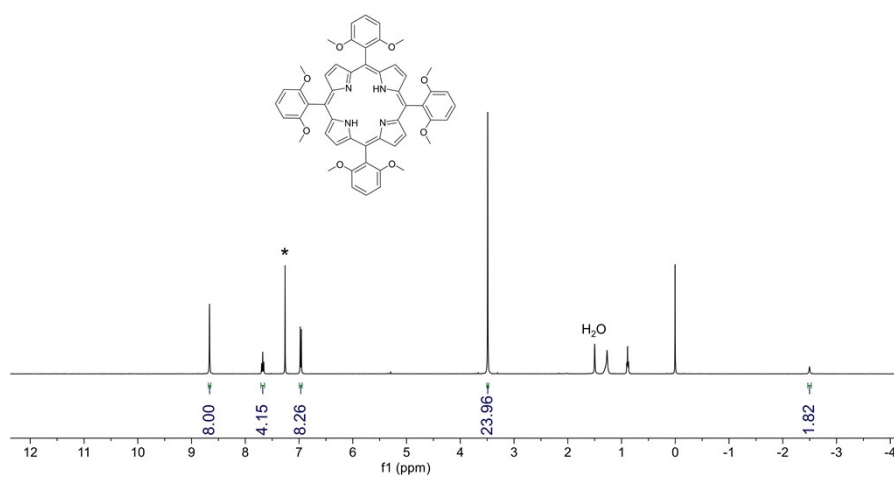


**Fig. S1** <sup>1</sup>H NMR spectrum of **a** in CDCl<sub>3</sub>. The solvent residue peak is labeled (\*).

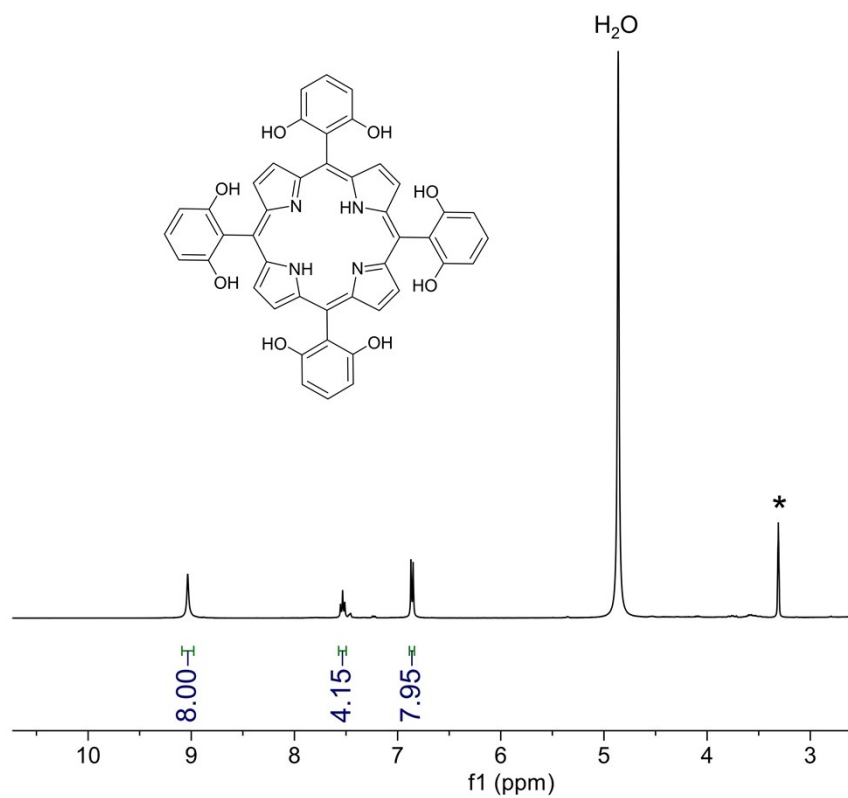


**Fig. S2** <sup>1</sup>H NMR spectrum of **b** in CDCl<sub>3</sub>. The solvent residue peak is labeled (\*).

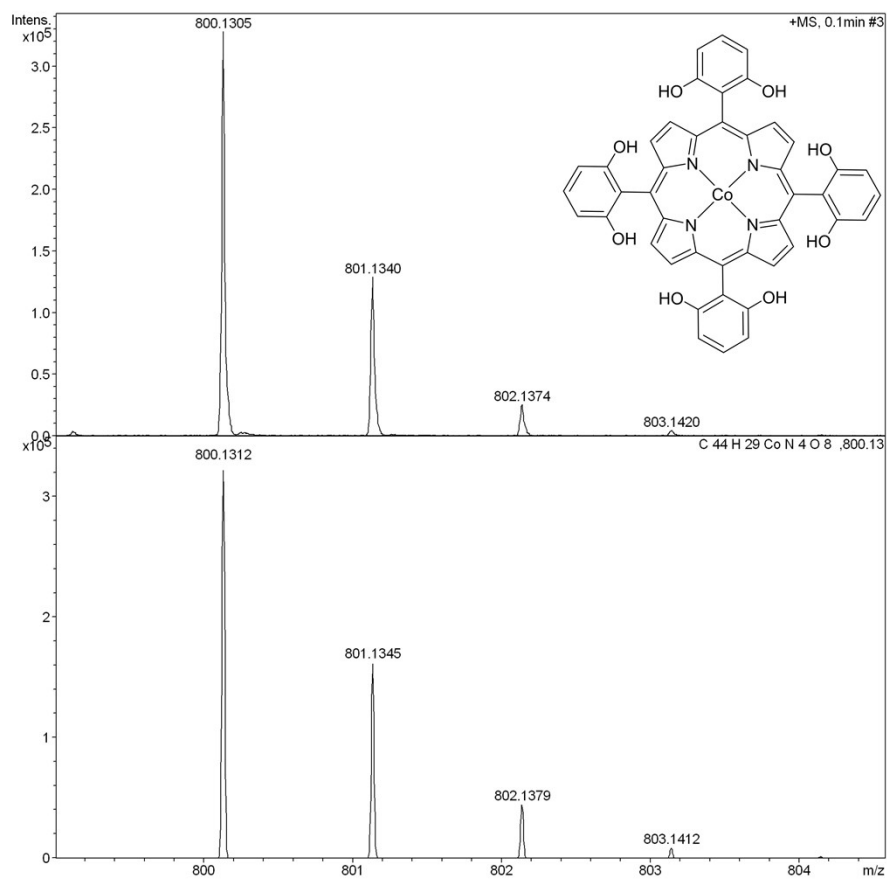


**Fig. S3** HRMS of **c** in methanol. The ion at a mass-to-charge ratio of 800.1306 matches the calculated value of 800.1312 for the monocation of  $[M + H]^+$ .

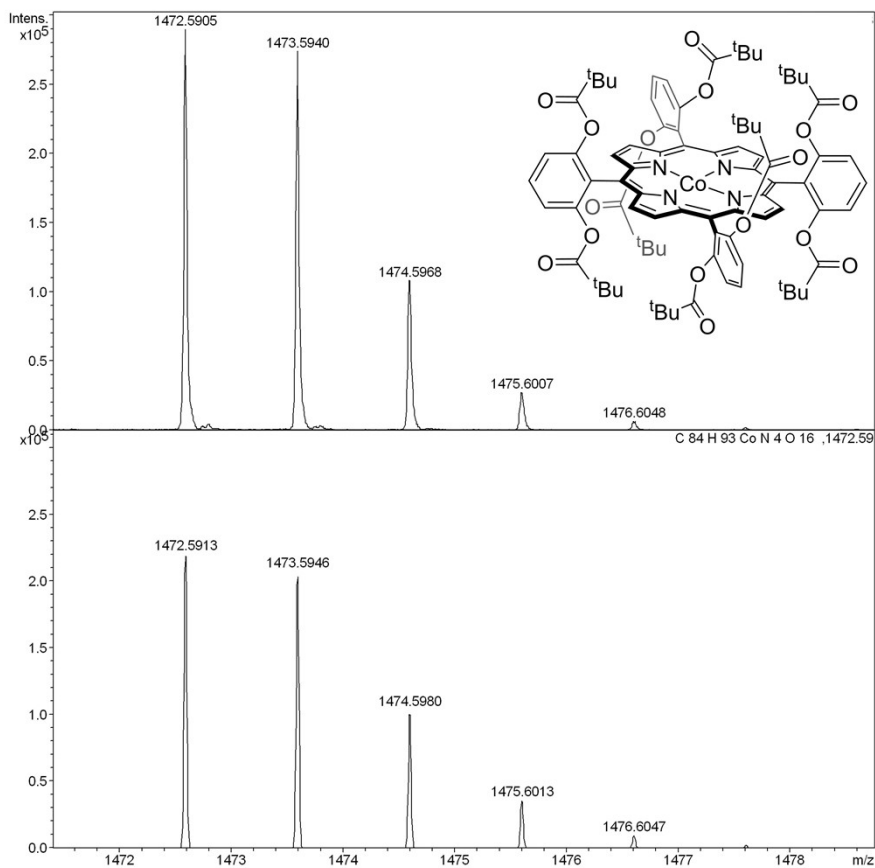


**Fig. S4** HRMS of **1** in methanol. The ion at a mass-to-charge ratio of 1472.5905 matches the calculated value of 1472.5913 for the monocation of  $[M + H]^+$ .

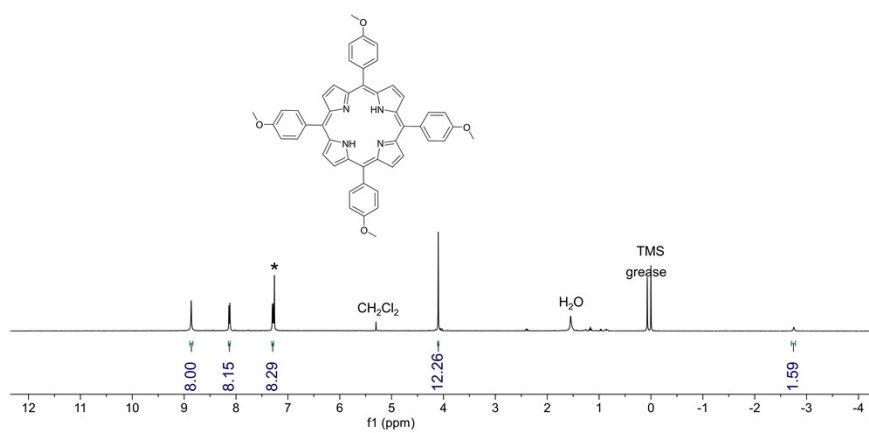


**Fig. S5** <sup>1</sup>H NMR spectrum of **d** in CDCl<sub>3</sub>. The solvent residue peak is labeled (\*).

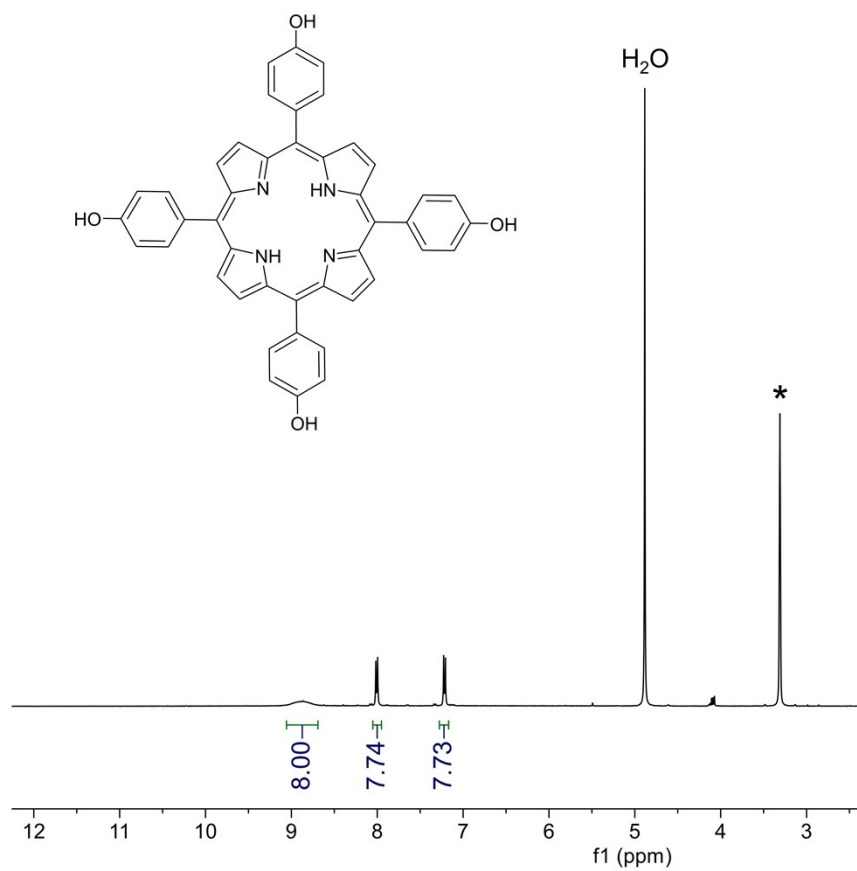


**Fig. S6** <sup>1</sup>H NMR spectrum of **e** in CDCl<sub>3</sub>. The solvent residue peak is labeled (\*).

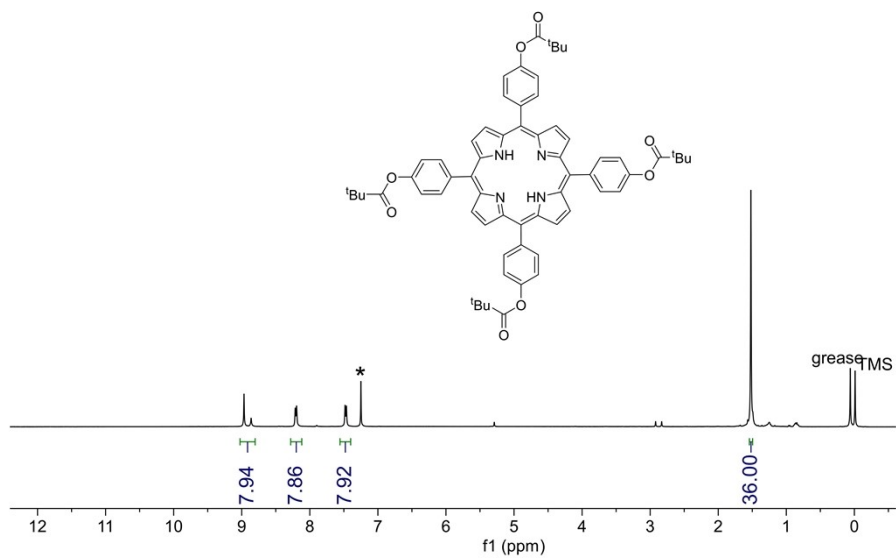


**Fig. S7** <sup>1</sup>H NMR spectrum of **f** in CDCl<sub>3</sub>. The solvent residue peak is labeled (\*).



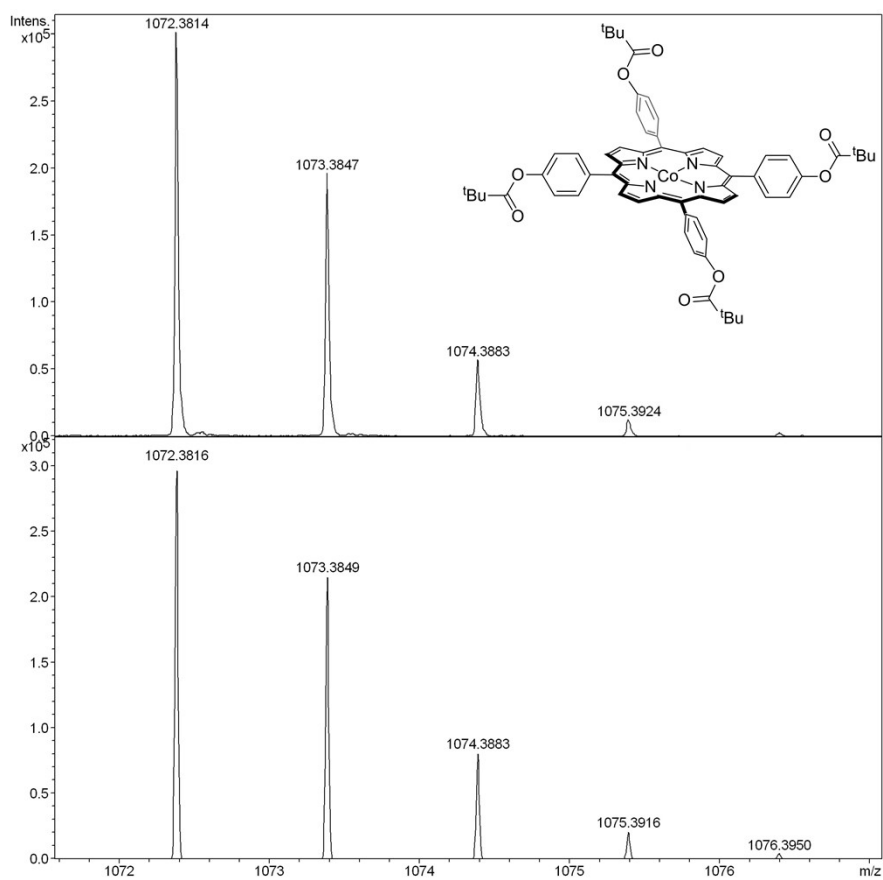


**Fig. S8** HRMS of **2** in methanol. The ion at a mass-to-charge ratio of 1072.3814 matches the calculated value of 1072.3816 for the monocation of  $[M + H]^+$ .

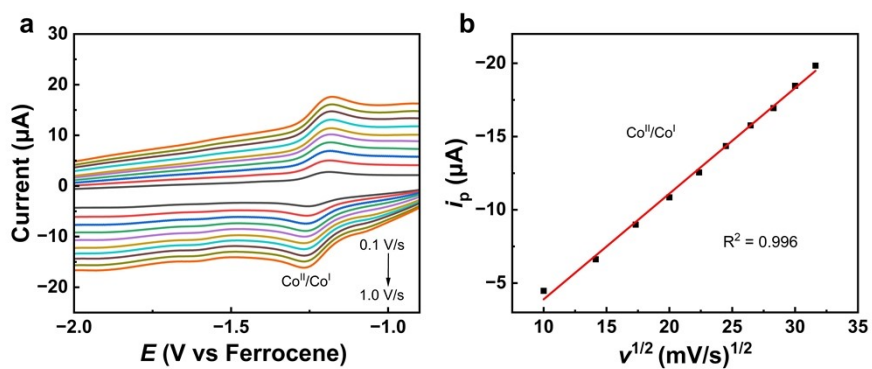


**Fig. S9** (a) CVs of 0.5 mM **1** under argon with different scan rates in DMF. (b) Plots of currents of  $\text{Co}^{\text{II}}$  reduction peaks versus the square root of scan rates. Conditions: 0.1 M  $\text{Bu}_4\text{NPF}_6$  and GC electrode.

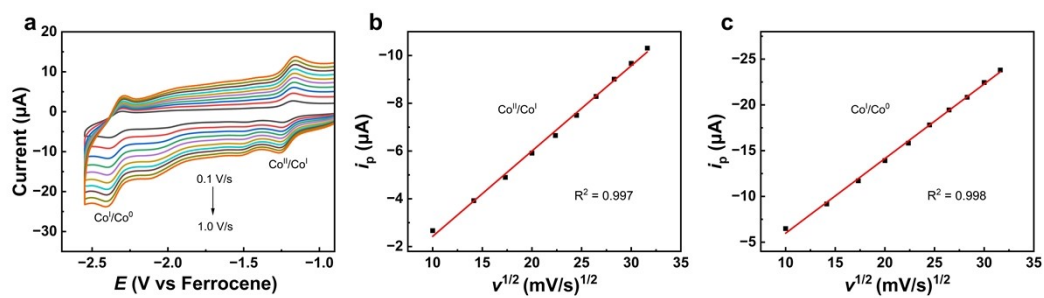


**Fig. S10** (a) CVs of 0.5 mM **2** under argon with different scan rates in DMF. (b) Plots of currents of  $\text{Co}^{\text{II/I}}$  and  $\text{Co}^{\text{I/0}}$  reduction peaks versus the square root of scan rates. Conditions: 0.1 M  $\text{Bu}_4\text{NPF}_6$  and GC electrode.

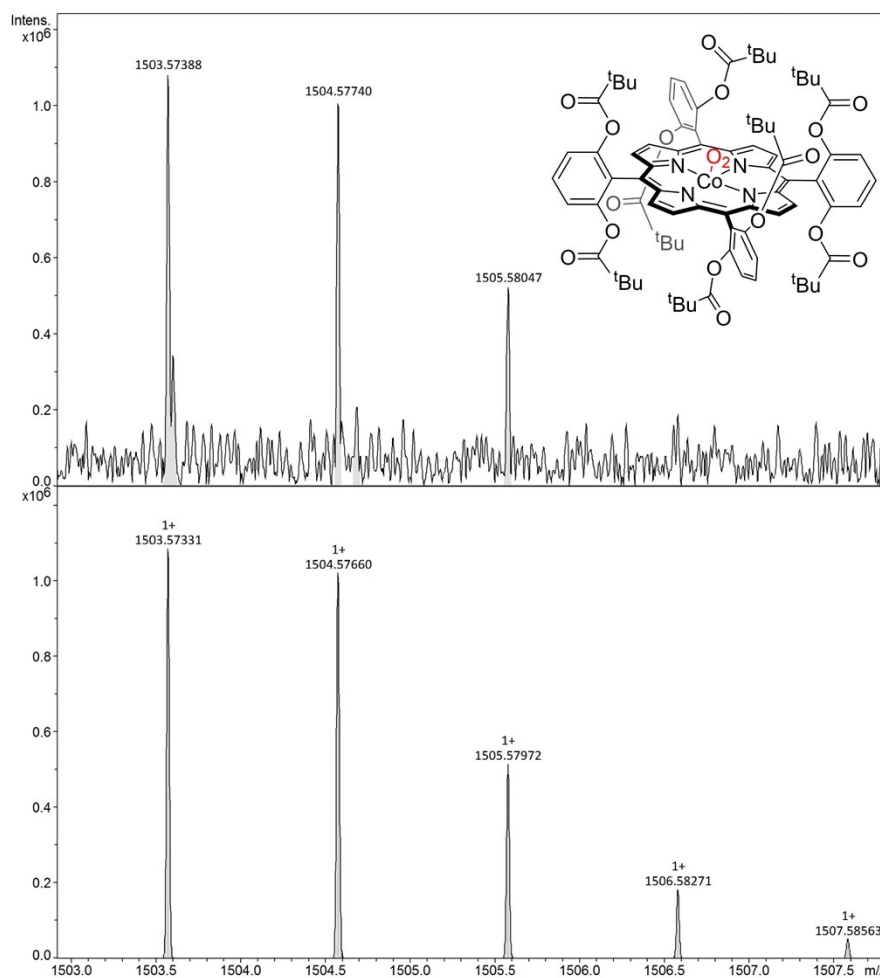


**Fig. S11** HRMS of O<sub>2</sub>-treated **1** in methanol. The ion at a mass-to-charge ratio of 1503.57388 matches the calculated value of 1503.57331 for the monocation of [M]<sup>+</sup>.

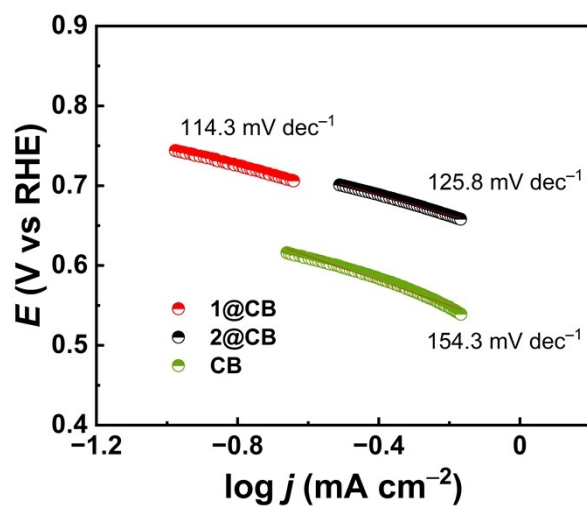


**Fig. S12** Tafel plots derived from LSV curves.

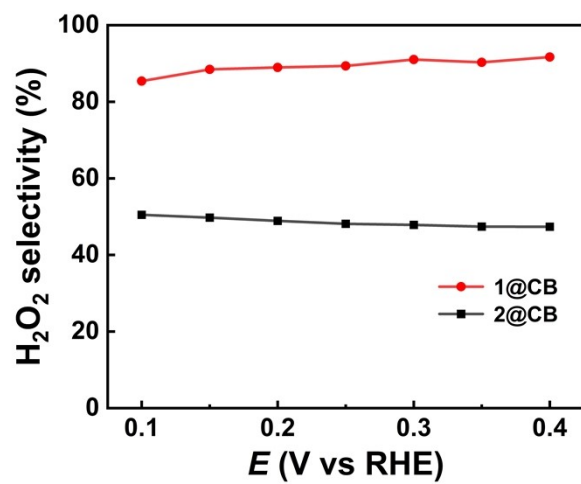


**Fig. S13** H<sub>2</sub>O<sub>2</sub> selectivity with 1@CB and 2@CB.

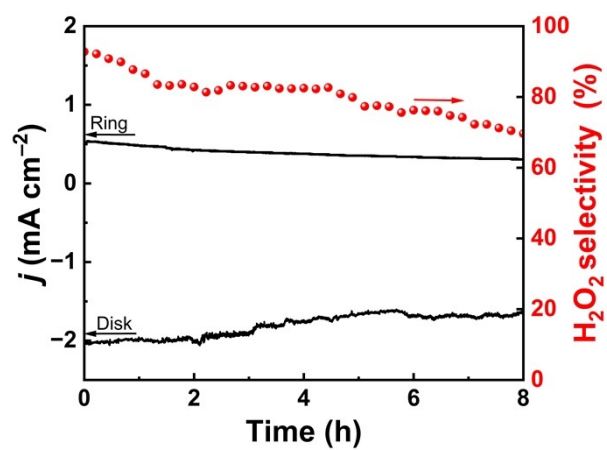


**Fig. S14** RRDE stability evaluation of **1@CB** at a fixed disk potential of 0.3 V (vs RHE).

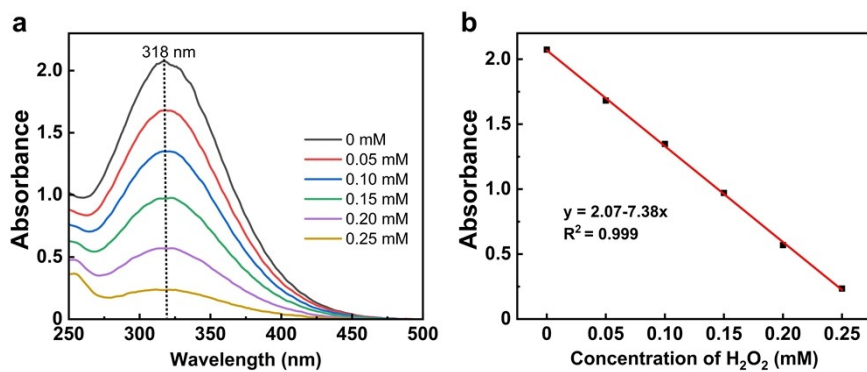


**Fig. S15** (a) UV-vis absorbance spectra containing different concentrations of H<sub>2</sub>O<sub>2</sub>.

(b) Calibration graph for different concentrations of H<sub>2</sub>O<sub>2</sub>.



**Table S1** Crystal data and structure refinement parameters of **1** and **2**.

<b>Complex</b>	<b>1</b>	<b>2</b>
molecular formula	C <sub>84</sub> H <sub>94</sub> CoN <sub>4</sub> O <sub>17</sub>	C <sub>64</sub> H <sub>60</sub> CoN <sub>4</sub> O <sub>8</sub>
formula wt. (g mol <sup>-1</sup> )	1490.56	1072.09
temperature (K)	153	190
radiation (λ, Å)	0.71073	1.34139
crystal system	Orthorhombic	Triclinic
space group	<i>Cmcm</i>	<i>P</i> $\bar{1}$
<i>a</i> (Å)	13.907(3)	9.8827(18)
<i>b</i> (Å)	23.347(4)	16.038(3)
<i>c</i> (Å)	25.011(4)	19.204(3)
$\alpha$ (°)	90	77.886(7)
$\beta$ (°)	90	86.561(7)
$\gamma$ (°)	90	82.747(7)
volume (Å <sup>3</sup> )	8121(2)	2950.3(9)
<i>Z</i>	4	2
$\rho_{\text{calcd}}$ (g cm <sup>-3</sup> )	1.219	1.207
$\mu$ (mm <sup>-1</sup> )	0.279	1.884
<i>F</i> (000)	3156.0	1126.0
crystal size (mm <sup>3</sup> )	0.20 × 0.10 × 0.10	0.20 × 0.10 × 0.10
2 theta range (°)	3.778 to 50.19	4.096 to 110.064
reflections collected	67886	40473
independent reflections	3854 [ <i>R</i> (int) = 0.1324]	10975 [ <i>R</i> (int) = 0.0932]
completeness	99.7%	97.4%
goodness-of-fit on <i>F</i> <sup>2</sup>	1.081	1.040
final <i>R</i> indices [ <i>R</i> > 2σ ( <i>I</i> )]	<i>R</i> <sub>1</sub> <sup>a</sup> = 0.1167 <i>wR</i> <sub>2</sub> <sup>b</sup> = 0.2773	<i>R</i> <sub>1</sub> <sup>a</sup> = 0.1003 <i>wR</i> <sub>2</sub> <sup>b</sup> = 0.2677
<i>R</i> indices (all data)	<i>R</i> <sub>1</sub> <sup>a</sup> = 0.1542 <i>wR</i> <sub>2</sub> <sup>b</sup> = 0.3106	<i>R</i> <sub>1</sub> <sup>a</sup> = 0.1841 <i>wR</i> <sub>2</sub> <sup>b</sup> = 0.3331
largest diff. peak and hole (e Å <sup>-3</sup> )	0.54 and -0.38	0.64 and -0.59

$${}^a R_1 = \frac{\sum ||F_o| - |F_c||}{\sum |F_o|}, {}^b wR_2 = \left\{ \frac{\sum [w(F_o^2 - F_c^2)^2]}{\sum [w(F_o^2)]} \right\}^{0.5}$$

### Supporting References:

- 1 *APEX v2009*, Bruker AXS, Madison, WI, 2009.
- 2 G. M. Sheldrick, *SADABS, 2008/1*, University of Göttingen, Göttingen, Germany, 2008.
- 3 G. M. Sheldrick, *Acta Crystallogr., Sect. A: Found. Crystallogr.*, 1990, **46**, 467-473.
- 4 G. M. Sheldrick, *Acta Crystallogr., Sect. A: Found. Crystallogr.*, 2008, **64**, 112-122.